Electron Transport in Particulate ZnO Electrodes: A Simple Approach

Volker Noack, Horst Weller, and Alexander Eychmüller*

Institute of Physical Chemistry, University of Hamburg, Bundesstrasse 45, 20146 Hamburg, Germany

Received: January 9, 2002; In Final Form: March 18, 2002

The charge transport in nanoparticulate ZnO layers held at different potentials was studied by analyzing the anodic transient photocurrents. The electrodes used in the electrochemical cell consisted of ZnO films coated onto conductive ITO substrates. In these experiments, three contributions to the photocurrent could be distinguished which were ascribed to a fast initial charge transport, a slow transport via deep trap states, and a transport via conduction band states or shallow traps. For the latter process, a simple phenomenological model is derived which enables a representation of the transients using only three parameters. These parameters account for the transport through the particulate ZnO layer, for the transport through the substrate, and for the amount of charge initially being present. The decay of the photocurrent signal is limited by transport through the ITO and the electrical connections, whereas the rise reflects mainly the transport through the ZnO itself. If the experimental results are interpreted in terms of a diffusion according to the theory of a random walk, the effective diffusion constant for the electron transport through the ZnO film held at positive potentials is calculated to be 1.7×10^{-4} cm^2/s which is in good agreement with diffusion constants reported for particulate electrodes.

Introduction

In current research on photovoltaics and photocatalysis, nanoparticulate electrode materials have taken their place because they offer a large internal surface area with respect to the macroscopic dimensions of such electrodes.[1,2] Especially, transparent oxide semiconductors such as TiO_2, ZnO, and SnO_2 became most common as substrates for sensitized solar cells because of their high stability and their low production costs. Because most applications require properties which are optimized with respect to the charge transport, it is of major importance to gain detailed information about the basic processes involved in both electron and hole transport in nanostructured materials. For this purpose, electrochemical methods have proven to be a valuable tool by which the temporal evolution of a current of (photogenerated) charge carriers is monitored with respect to the potential applied. The experimental techniques most promising are the recording of transient photocurrents,[3−5] impedance spectroscopy,[6] and intensity-modulated photocurrent spectroscopy.[7−9] In comparison to the latter methods, the interpretation of transient photocurrents is rather complex because the system is perturbed strongly by the illuminating light source (which usually is a laser). However, a lot of excellent work has been carried out in this field to describe the processes occurring in TiO_2 electrodes. Hence, it was possible to describe the electron transport in transient photocurrent experiments in terms of a diffusion process by solving the diffusion equations analytically[4] or numerically[5] as well as in terms of a random walk by performing Monte Carlo simulations.[10,11] It is thus remarkable that only few publications deal with the respective experiments using particulate ZnO electrodes because this material has similar electrochemical and optical properties as TiO_2 and can be obtained in the gram scale by simpler (and less expensive) preparative routes.[12,13] The cause for this obvious lack of studies in this field might depend on the complex behavior of the transient photocurrents of ZnO electrodes, aggravating a description within the framework of conventional transport theory.

To describe the electron transport through porous layers, the approaches mentioned above require additional knowledge of the underlying processes. This information is needed in the calculations as boundary or initial conditions of the respective experimental setup and might thus be relevant only for the specific system. Furthermore, these techniques require a considerable mathematical or computational effort for the evaluation of the transient currents. It would be desirable to refer to a simple model which is based on less assumptions and provides an easy way for the interpretation of the experimental findings. The aim of this study is to present such a mathematically simple approach for the evaluation of the transient photocurrents in particulate electrodes and hence to gain information about the processes involved in an electron transport through nanostructured ZnO films coated on a standard ITO substrate.

Experimental Section

Preparation of the ZnO Particles. The ZnO colloid was prepared according to the method described by Spanhel and Anderson:[13] A suspension of 11.0 g of zinc acetate dihydrate (98+ %, Aldrich) in 500 mL of ethanol (p. a., Merck) was refluxed for 1 h. Hereafter, 300 mL of the solvent was removed by distillation and replaced by the same amount of fresh ethanol. To the suspension was added 2.9 g of lithium hydroxide monohydrate (p. a., Fluka) in an ultrasonic bath at 0 °C. Finally, the resulting transparent solution was filtered through a 0.1 μm glass fiber filter.

To obtain a stable particulate sample from this solution, a method described by Hoyer was employed:[14] The solution was heated and mixed at 60 °C with a small amount of deionized water (Milli-Q_{PLUS}, Millipore). A colorless precipitate was formed which was subsequently separated from the supernatant

* To whom correspondence should be addressed. E-mail: eychmuel@chemie.uni-hamburg.de.

10.1021/jp0200270 CCC: $22.00
Published on Web 07/31/2002

solution by centrifugation. For purification, the precipitate was washed with a mixture of ethanol and water (95:5) and centrifuged again. After repeating the last two steps four times, the precipitate was suspended in a few milliliters of ethanol using an ultrasonic bath.

Preparation of the Electrodes. Conductive ITO substrates (25×25 mm^2, 25 Ω/sq, Schott) were cleansed in a boiling solution containing 5 vol. % of a cleaning agent (Extran MA01 alkaline, Merck) and rinsed with water. Onto the dried ITO substrate, the diluted precipitate was spin-coated using a home-built apparatus (rotation speed: 3300 rpm). For the removal of residual solvent, the sample was heated in a furnace at 100 °C for 5 min. The thickness of the ZnO film obtained in one coating step has shown to be strongly dependent on the viscosity of the employed colloidal solution. To obtain films with different thicknesses, the coating process was repeated several times. A stylus profilometer (Alphastep 200, Tencor Instruments) was used to measure the thickness achieved. Finally, the sample was annealed in a furnace for 30 min at 300 °C. A characterization of the thus obtained ZnO films is given in a previous publication.[15] The resulting ZnO particles are spherical in shape and have an average diameter of 6 nm. As confirmed by polarographic analysis as well as absorption spectroscopy, the ZnO films exhibit a space filling of 60%.

For the preparation of the electrodes, the substrate was cut into four pieces. To obtain an electrical contact with a good conductivity between the ITO and the connecting wires, the ZnO film was scraped off in one corner of the sample with a scalpel, and a copper wire was attached using an Ag-containing epoxy resin (3021, Epoxy-Produkte). Finally, the contact area was sealed with an insulating resin (Scotchcast No. 10/XR5241, 3M).

Photoelectrochemical Measurements. The ZnO/ITO electrodes were used as working electrodes in an electrochemical cell with a glassy carbon counter electrode and an Ag/AgCl/3 M NaCl reference electrode (+207 mV vs SHE). In this study, all potentials are reported against the Ag/AgCl/3 M NaCl electrode. The experiments were performed under short circuit conditions using a home-built potentiostat with a low input impedance (<1 Ω) and a potential rise time of less than 300 ns (depending on the capacitance of the respective sample). The electrochemical cell was equipped with a quartz window. As electrolyte solution, an aqueous HCl/borate buffer solution (pH 8, Merck) containing 1 M $LiClO_4$ (p.a., Fluka) and 30 vol. % ethanol was chosen. The electrolyte solution was deaerated with high purity nitrogen for at least 20 min before electrochemical studies were conducted. The nitrogen was allowed to flow over the solution surface during experiments.

The transient photocurrents were recorded with an oscilloscope (54522A Oscilloscope, Hewlett-Packard). As exciting light, the frequency-multiplied line of a Nd:YAG laser (SL804T, Spectra Laser Systems, Polytec) was used with a wavelength of 266 nm and a pulse duration of 10 ns. The beam was broadened using a quartz lens in order to ensure the illumination of the whole area of the working electrode. A Rm-3700 universal radiometer equipped with a RjP-375 energy probe (Laser Probe Inc.) was employed to monitor the light intensity. Unless not otherwise stated, the laser beam was attenuated to an energy density of 30 μJ/cm^2 per pulse. It was confirmed by performing experiments at higher laser intensities that the total charge flown varied linearly with the intensity up to a pulse energy of 80 μJ/cm^2; hence, only monophotonic processes have to be considered. In all experiments the electrode was illuminated by the laser light from the front side (i.e., not from the substrate side).

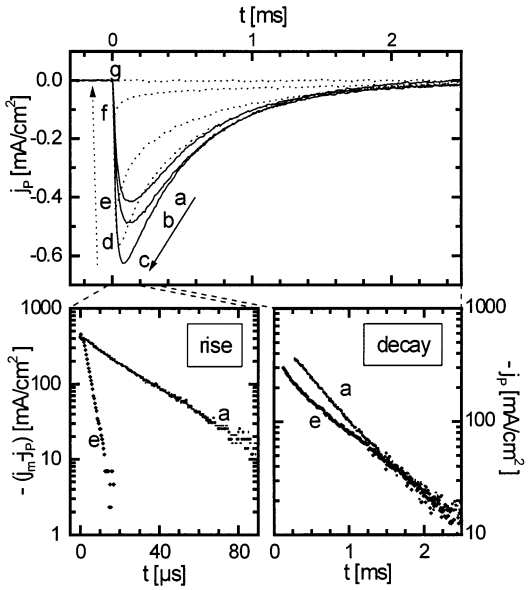

Figure 1. Transient photocurrent densities of a particulate ZnO film having a thickness of 1,1 μm. The transients were obtained for the electrode being held at a potential of 0 mV (a, solid line), −50 mV (b), −200 mV (c), −250 mV (d, dotted line), −300 mV (e), −400 mV (f), and −550 mV (g), respectively. Upper part: Representation of the experimental data on a linear scale. The arrows act as guides denoting the evolution of the transients by shifting the potential in the negative direction. Lower part: Two different logarithmic representations of curves a and e in the upper part. (right side: photocurrent density of the decaying part of the signal on a logarithmic scale; left side: difference between the photocurrent density and the maximum current density for the rising part of the transient signal on a logarithmic scale).

For each potential, the photocurrents were recorded on three different time scales in order to improve the resolution for the rise and the decay of the transient current. The respective photocurrent transients were obtained at room temperature by averaging 16 measurements with an intermission of several seconds between the two consecutive measurements. The dc offset currents were removed from the data curves by subtracting the current transients recorded similarly but without illumination. The photocurrents were corrected with respect to the actual area of the ZnO film in order to obtain the current densities.

Because in different batches the properties of the ZnO colloid might change slightly, the interpretation of the transient photocurrents is done only for electrodes made from the same batch. Additionally, before and after exposure to the laser light, absorption spectra of the electrodes were taken and cyclovoltammetric measurements were performed in order to ensure that the samples had not suffered damage during the experiments.

Results and Discussion

In Figure 1, the transient photocurrent densities j_P are given for a particulate ZnO electrode with a thickness of 1.1 μm at different potentials applied. In the upper part of Figure 1, the photocurrent data are depicted on a linear scale. For all potentials, the anodic current exhibits a fast rise until a maximum of the photocurrent is reached, followed by a slower decrease.

When positive potentials up to 0 mV were applied (curve a), 130 μs after the laser pulse the maximum current density is observed, and the shape of the transient is independent of the actual potential. For particulate ZnO electrodes having a thickness of less than 1 μm, Hotchandani and Kamat reported a rise time of the transient photopotential of 150 μs which corresponds nicely with our value.[16]

When the potential is shifted from 0 mV in the negative direction, two major effects on the photocurrent are observed. First, the rise of the transient becomes faster. At potentials negative of −350 mV, the rise of the signal cannot be resolved properly with the potentiostat used in these measurements (i.e., the rise time was about 300 ns or faster). Second, the current density in the maximum increases peaking at −200 mV. If an even more negative potential is applied, the current density in the maximum decreases again. At potentials negative of −600 mV, no current at all is detected. A similar complexity of the photocurrent transients with respect to the potential applied was observed for particulate electrodes consisting of ZnO [3] and of TiO_2 [5]

However, in our case, the potential applied affects only the rise of the current transient and the maximum current; for the decay of the current transient, no effect of the potential applied is observed. The time constant of this decay was found to be about 500 μs.

When the potential applied is shifted in the negative direction, the energy of the Fermi level of the semiconductor electrode is raised. In distinction from macroscopic semiconductors, no band bending of the conduction and valence bands across the film is apparent because a major potential drop cannot be established due to the screening by the electrolyte solution interpenetrating the porous structure. Therefore, the external voltage applied directly affects the occupation of the electronic states in the semiconductor particles. Thus, the shift of the Fermi level toward higher energies corresponds to a process in which electronic states with a higher energy are filled via the back contact.

To specify the temporal evolution of the photocurrents, different logarithmic representations were chosen for the rise (Figure 1, lower part, left side) and the decay (right side) of the transients. As can be seen from the diagram on the right-hand side, both photocurrent data curves decay exponentially in time. For the transient obtained at a potential of 0 mV, this agreement is excellent. Consequently, in contrast to particulate TiO_2 electrodes[10] and amorphous solids,[17] the model of a dispersion of the carrier transit times does not apply for the transport through the ZnO/ITO electrode held at positive potentials. However, for the photocurrents obtained at −300 mV, a deviation from the exponential behavior is observed within the first 200 μs. This might either indicate that the mechanism of a charge transport changes during the transport process or that more than one transport channel have to be considered within the first microseconds after the laser pulse.

In the diagram on the left side of the lower part of Figure 1, the respective rise of the photocurrent density is shown. To separate the decaying part of the transient from its build-up, a representation was chosen which is common for the analysis of saturation kinetics: Simply, the transient photocurrent j_P was subtracted from the maximum current j_m obtained for the respective potential. The resulting difference is plotted on a logarithmic scale. For both data curves, it is found that this difference evolves strictly exponentially in time indicating that the whole photocurrent signal can be explained by two coupled processes which evolve both exponentially in time.

The transients monitored in these experiments might not only depend on the particulate film itself but also on limitations by the remaining electrochemical system, i.e., the resistivity and the capacitance of the substrate, the electrolyte solution, the counter electrode, the connecting wires, and the potentiostat. A detailed analysis of the influence of the electrolyte solution and the laser intensity on the transient photocurrents will be given in a forthcoming paper.[18]

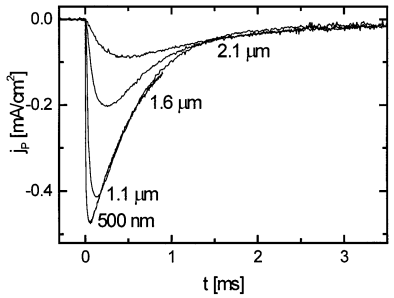

Figure 2. Transient photocurrent densities of particulate ZnO electrodes having different film thicknesses. The electrodes were held at a potential of +200 mV.

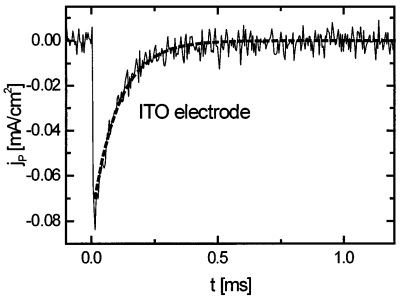

Figure 3. Transient photocurrent density of a blank ITO film (solid line), held at +200 mV. The laser pulse intensity was chosen to be 65 μJ/cm^2. The heavy dashed line represents a fit using a single-exponential function in order to describe the photocurrent decay of the ITO electrode.

To specify the contribution of the oxide particles, measurements were performed with samples having different thicknesses of the ZnO film. In Figure 2, the transient photocurrent densities are depicted which were obtained in these experiments with electrodes being held at +200 mV. It can be seen that the film thickness affects only the rise time of the photocurrent, whereas the decay characteristic remains almost unchanged (see below). From the absorption spectra, the extinction coefficient for the porous ZnO layer at a wavelength of 266 nm was calculated to be 4.8×10^5 cm^{-1} resulting in a penetration depth of 90 nm (corresponding to the depth where the incident light is attenuated to 1/e of its initial value). Thus, at this potential, all of our samples absorb the same number of photons per laser pulse, and the initial concentration profile of the electrons is the same for all samples examined. Consequently, the differences in the transient photocurrents of electrodes having different thicknesses are unlikely to be ascribed to nonlinearities in the charge transport. From these findings, it was concluded that the temporal evolution of the decaying current is governed rather by an electron transport through the substrate than by a transport through the ZnO layer of the electrode.

In Figure 3, the transient photocurrent density of a blank ITO electrode is depicted. Because the photocurrent of the bare ITO electrode was considerably small, the transient was recorded using a laser intensity of 65 μJ/cm^2 instead of 30 μJ/cm^2 used in all other experiments. The transient exhibits a fast initial rise of the anodic current which is faster than the rise time of the potentiostat. The fast rise is followed by a slower decay of the photocurrent signal. As can be seen from the fitted data (heavy dashed line), the decay is well described by a single-exponential function with a time constant of about 110 μs. To exclude a contribution of the measurement apparatus, photocurrent transients of a single crystalline silicon electrode without any substrate layer were recorded under the same conditions. These experiments have shown a clearly faster decay of the transient

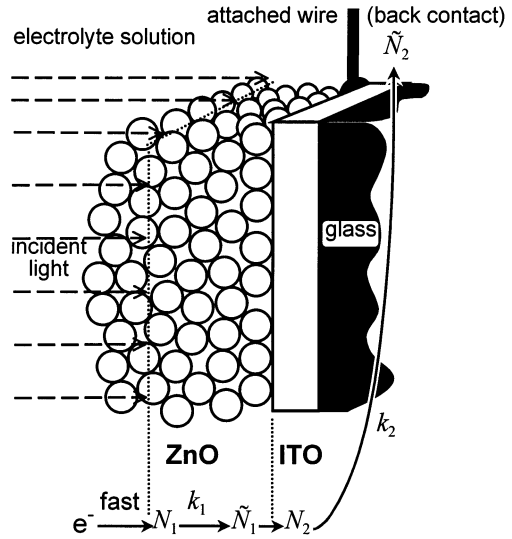

Figure 4. Schematic view of the charge transport through a particulate ZnO film on a conductive ITO substrate. The parameters N_1, $\tilde{N}_1$, N_2, $\tilde{N}_2$, k_1, and k_2 are referring to the phenomenological model as described in the text.

lasting only a few microseconds. Because the time constants for the decrease of the current transient in the bare ITO and in the ZnO/ITO electrode differ only by a factor of 5, they are of the same order of magnitude. Thus, no contradiction is given to the interpretation of the decay in terms of a transport through the substrate and the connections of the electrode.

Evaluation of the Transients. With these findings, a simple model was derived in order to describe the photocurrent transients in a purely phenomenological manner: Immediately after the laser pulse, a charge separation as well as recombination processes take place. In general, the recombination could be a geminate process (fluorescence or nonradiative recombination) as well as a process requiring more than two carriers (e.g., Auger recombination). However, from the intensity of the 266 nm laser pulse being 30 μJ/cm^2, the total number of photons incident on an area of 28 nm^2 (corresponding to the cross section area of the 6 nm particles) is calculated to be 11.3. With a penetration depth of 90 nm, the maximum number of photons absorbed within 6 nm (corresponding to the first layer of particles located in the outermost part of the electrode) can roughly be estimated to be 0.7. Thus, even under the strong illumination by the laser pulse, less than one electron−hole pair is generated per particle, and thus, mainly geminate recombination processes have to be considered. For particulate ZnO thin films, Hoyer reported fluorescence lifetimes being less than one microsecond.[14] Because the initial charge separation competes with such a geminate recombination, both processes have to take place on the same time scale and cannot be monitored in our photocurrent experiments because of the limitation of the experimental setup.

The situation obtained hereafter marks the starting point for the charge transport of the excited electrons. The net transport through the electrode is divided into two subsequent processes, one accounts for the charge transport through the nonilluminated part of the nanoporous ZnO (denoted by the index "1") and the other one for the transport through the ITO substrate to the back contact (denoted by the index "2").

The quantity observed in the measurements is the current which is monitored at the back contact. In general, a current is defined as the temporal change of the number N of electrons ($i(t) = e\ \mathrm{d}N/\mathrm{d}t$, with e being the elementary charge). Thus, it is useful to describe each transport process in terms of a change in the number of photoexcited electrons. The parameters used in this model are schematically shown in Figure 4. For the ZnO layer, the number of electrons adjacent to the illuminated side of the film is denoted as N_1, and the number of electrons inside the ZnO at the boundary to the ITO is denoted as $\tilde{N}_1$. The same notation was chosen for the ITO layer: N_2 refers to the excited electrons inside the substrate next to the ZnO layer, and $\tilde{N}_2$ denotes the electrons at the back contact.

For a good electrical contact between the ZnO and the ITO layer, the two quantities $\tilde{N}_1$ and N_2 referring to the electrons at both sides of the boundary must be equal ($\tilde{N}_1 = N_2$). (Because $\tilde{N}_1$ and N_2 denote only the point in which the charges are balanced, the exact position of this boundary might also be shifted into the adjacent layer of the ZnO. In this case, the contact resistance between the ITO and the ZnO would also contribute to the transport through the second regime. However, this would have virtually no implications for the interpretation of k_1.)

Because the rise of the transient photocurrent as well as the decay has been shown to follow a simple exponential relation with respect to the time, the apparent changes in the number of excited electrons at the respective locations inside the electrode are described by the following set of differential equations:

$$\frac{\mathrm{d}N_1}{\mathrm{d}t} = -k_1 N_1 \tag{1}$$

$$\frac{\mathrm{d}\tilde{N}_1}{\mathrm{d}t} = \frac{\mathrm{d}N_2}{\mathrm{d}t} = k_1 N_1 - k_2 N_2 \tag{2}$$

and

$$\frac{\mathrm{d}\tilde{N}_2}{\mathrm{d}t} = k_2 N_2 \tag{3}$$

k_1 and k_2 are rate constants referring to the temporal evolution of the current. As the electrons are instantaneously withdrawn at the back contact of the electrode, the transient photocurrent is given by $i_P(t) = \mathrm{e}\ \mathrm{d}\tilde{N}_2/\mathrm{d}t = \mathrm{e}\ k_2 N_2(t)$.

Equations 1−3 are found in textbooks because they describe also the kinetics of two coupled chemical reactions both being of first order. To solve this set of linear differential equations, one has to specify the boundary conditions which are the respective numbers of excited electrons being initially present. For the electrons adjacent to the illuminated part of the ZnO, $N_1(t = 0)$ equals the numbers of excited electrons $N_1{}^0$ as provided by the fast initial charge separation. Because the rest of the electrode is not illuminated by the laser, the respective initial conditions are $\tilde{N}_1{}^0 = N_2{}^0 = \tilde{N}_2{}^0 = 0$.

By following standard procedures in order to solve this set of equations,[19] the transient photocurrent is obtained. Because the total current scales with the electrode area A, it is convenient to use the current density instead. Thus, the total number $N_1{}^0$ of photoexcited electrons initially present is preferably replaced by the area density $n_1{}^0$ of these electrons (i.e., $n_1{}^0 = N_1{}^0/A$). Accordingly, the photocurrent density j_P (t) at the back contact is expressed as

$$j_P(t) = \frac{e}{A} k_2 N_2(t) = \frac{e n_1{}^0}{(k_2{}^{-1} - k_1{}^{-1})} [\exp(-k_2 t) - \exp(-k_1 t)] \tag{4}$$

Because the number $N_1{}^0$ of conduction band electrons initially present in the ZnO accounts only for the absolute magnitude of the current transient, it is possible to describe the temporal evolution of the photocurrent using only two parameters, k_1 and

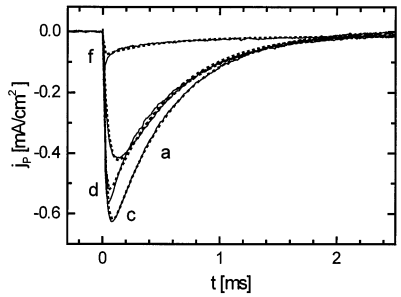

Figure 5. Transient photocurrent densities of a ZnO electrode (solid lines) in comparison with the simulated transients (dotted lines) obtained by using a fit according to the phenomenological model (eq 4). The curves are denoted as shown in Figure 1 (a: 0 mV; c: −200 mV; d: −250 mV; f: −400 mV).

k_2. It can be easily seen that the larger of these constants is responsible for the rise of the current, whereas the smaller one accounts for the decay. If one constant is larger by several orders of magnitude than the other, one might virtually observe an instantaneous current followed by a decay according to the slower transport process.

Figure 5 depicts a comparison between the photocurrents in Figure 1 and the simulated curves obtained by fitting the parameters in eq 4 to the transients. It is seen that at most potentials applied the phenomenological model describes the shape of the photocurrent densities sufficiently well. Small deviations from the behavior predicted by eq 4 are found only in the first microseconds after the laser pulse and at even longer times than shown. For the deviation appearing immediately after the laser flash, the current as described by the model is smaller than the actual transient. Thus, a small amount of the charge transported through the electrode is not accounted for by the simplified model. This difference increases by increasing the negative potential. The second deviation is observed only at potentials positive of −150 mV indicating an additional transport process being slower by more than 1 order of magnitude. In this process, a considerable amount of the electrons are found to reach the back contact at longer times. To account for these contributions to the total photocurrent, additional parameters would be required for a refinement of the simple model. However, by introducing new parameters, the correlation between the fitting parameters increases strongly denoting a loss of the physical significance of the refined model. Furthermore, the fitting procedure itself is problematic because of the very low signal intensity of the currents flown at longer times. Thus, it is more reasonable to evaluate the additional current components in terms of a qualitative analysis of the observations made.

In Figure 6, the parameters obtained by fitting eq 4 to the photocurrent transients are collected for a bare ITO electrode and for a ZnO sample having a film thickness of 1.1 μm. The lower part shows the preexponential factor $n_1{}^0$ of a ZnO/ITO electrode (diamonds) and of a bare ITO electrode (crosses) as a function of the potential applied. As can be calculated by integration of eq 4, $n_1{}^0$ corresponds to the total number of electrons which are transported through the electrode according to the simple model. For the bare ITO film, $n_1{}^0$ is smaller by 2 orders of magnitude than for the ZnO/ITO electrode. For the ZnO sample held at positive potentials, the total charge is independent of the exact electrode potential. As the potential is shifted in the negative direction, $n_1{}^0$ increases peaking at −150 mV and thereafter decreases. At a potential of roughly −500 mV, no charge is transported according to the simplified model. The decrease of the photocurrent at negative potentials is in

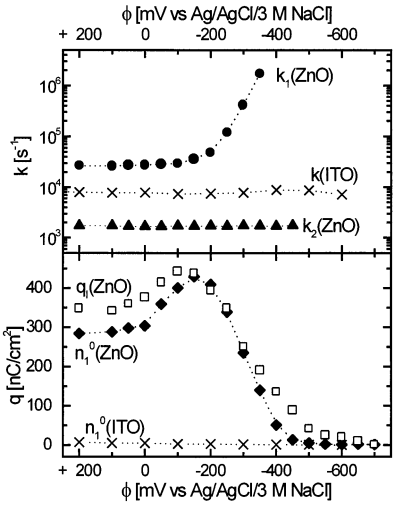

Figure 6. Parameters obtained by fitting eq 4 to the photocurrent transients of a bare ITO substrate (crosses) and of a particulate ZnO electrode (solid symbols) having a thickness of 1.1 μm. The open squares in the lower part denote the total charge flown through the ZnO electrode as a result of an integration of the respective photocurrent transients.

good agreement with the decrease observed for ZnO electrodes in experiments on stationary photocurrents.[9,14,16] However, no peaking of the photocurrent was apparent in the stationary measurements. The transport of the electrons through the ZnO layer takes place via empty states with the lowest energy. By shifting the potential applied in negative direction, electronic states with a higher energy are occupied. If the energy of this Fermi level is chosen to be somewhere in the band gap, the number of electronic states which are occupied during the charge transport is low and virtually the same for all Fermi levels because of the low density of states. Consequently, no changes in the photocurrent are observed. By shifting the Fermi level close to the conduction band, the number of empty states which are actually occupied in the transport process increases, and an effect on the transients is expected. As electronic states or shallow traps close to the conduction band are filled via the back contact, the gradient in the electrochemical potential across the ZnO decreases and thus the initial charge separation is retarded. As a consequence, the photogenerated charge carriers remain inside the illuminated part of the ZnO film for longer times and additional recombination processes can take place. Because the latter compete with a charge transport, the photocurrent decreases until it vanishes completely if the potential of the conduction band is applied. From the drop of $n_1{}^0$, the potential corresponding to the energy of the conduction band for the particulate ZnO film is found to be about −500 mV.

In addition to $n_1{}^0$, in Figure 6, the total charge flown q_I as obtained by integrating the photocurrent transient is depicted (open symbols). If the transport of all photogenerated charge carriers is fully described by the model chosen, the integral charge and the parameter $n_1{}^0$ are expected to be equal. Thus, q_I might serve as an indicator in order to check the limitations of the simplified model. Both data curves exhibit a similar shape but diverging slightly at positive potentials and at potentials between −300 and −600 mV. The deviation at positive potentials is in agreement with the current observed at long times after the laser pulse (see above). Thus, it should be based on a slow transport of the electrons moving through the electrode. A second process accounts for the observed difference at potentials between −300 and −600 mV. This deviation arises from contributions to the photocurrent transients which takes

place only in the first microseconds after the laser pulse (cf. Figure 5). By shifting the potential of the electrode in the negative direction, this fast component of the photocurrent is the last to vanish. However, this current component has to be distinguished from an exponentially decaying current spike which was observed by some authors for particulate oxides. This initial current was interpreted in terms of a fast electron transport via shallow traps,[3] as a photocurrent due to reflected excitation light entering the cell from the backside,[11] or as a reorganization of the electrolyte solution which follows a fast initial movement of the photogenerated electrons caused by electrostatic repulsion.[4,5] A similar decay was observed by Hotchandani and Kamat in measurements of transient photopotentials at particulate ZnO electrodes which was explained by the fast initial charge separation.[16] For the ZnO/ITO electrodes described in our study, such an initially decaying current was also observed in some cases. However, the current spike in our experiments was significantly diminished by employing a potentiostat with an increased time resolution. Thus, in our case, the current spike was clearly an artifact of the measurement apparatus itself.

In the upper part of Figure 6, the rate constants k_1 and k_2 are depicted on a logarithmic scale. The parameter k_2 exhibits no dependence of the potential applied. The same observation is made for the bare ITO electrode. Nevertheless, there is a difference in the mean value for the rate constant of the bare ITO being 8500 s^{-1} and for k_2 of the ZnO coated electrode being only 1700 s^{-1}. Additionally, no dependence was found for k_2 of the ZnO/ITO electrodes or for the rate constant of the bare ITO electrode from the composition of the electrolyte solution, whereas k_1 was strongly affected under these conditions (as will be shown in a forthcoming paper[18]). The only parameter which has shown to have a distinct effect on the decay of the photocurrent in both systems was the electrode area: by increasing the size of the area, the decay became slower for the ITO as well as for the ZnO/ITO samples. These similarities show the close relationship between the fit parameter k_2 and the charge transport through the ITO layer. Thus, several different quantities might contribute to k_2: the resistance of the conducting adhesive, the sheet resistance of the ITO, and the contact resistance between the ITO and the ZnO layer. However, the correct identification of these contributions is only of minor interest for this study, because this underlying mechanism has no effect on the transport through the nonilluminated part of the electrode. Thus, the true origin of the apparently different numbers of k_2 and the rate constant of bare ITO cannot be unambiguously given here; it might arise from different geometries of the electrode area, different charge carrier concentrations, or simply from the annealing process, which might change the composition of the surface and thus the contact resistance or the conductivity of the ITO itself.[20]

Hence, the ITO substrate and the electrical connections limit the rate of the charge transport through the ZnO/ITO electrode. A similar conclusion was drawn by de Jongh and co-workers from intensity-modulated photocurrent spectroscopy experiments:[9] These authors report a characteristic time for the charge transport in particulate ZnO electrodes which decreases by a factor of 10 after changing the substrate from ITO to gold, whereas no such behavior was observed for TiO_2 electrodes. To overcome this contribution of the ITO, it thus might be useful to employ other electrode materials as substrates rather than the most popular ITO.

For the second parameter, k_1, the effect of the potential applied is significantly different: At potentials being more positive than −150 mV, k_1 mainly remains unchanged having an average value of 27 000 s^{-1}. If the potential is shifted in the negative direction, k_1 increases by almost 2 orders of magnitude. Because at these potentials conduction band states of the ZnO particles are filled with electrons via the back contact, the effective density of conduction band electrons is raised, and thus, a faster transport of the photogenerated charge carriers toward the back contact might be expected to take place.

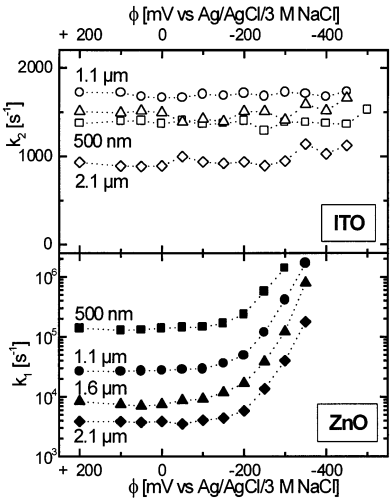

Figure 7. Fitting parameters k_1 (solid symbols) and k_2 (open symbols) for ZnO electrodes having different film thicknesses (500 nm, 1.1 μm, 1.6 μm, and 2.1 μm). These parameters describe the temporal evolution of the photocurrent signal according to the simple model.

In Figure 7, the rate constants k_1 and k_2 as determined by the fitting procedure are shown for samples having different thicknesses of the ZnO film. In the upper part, the rate constant k_2 for the charge transport through the substrate is given. In agreement with the data obtained for bare ITO electrodes, the potential applied has no influence on k_2 for all samples shown. The average values for k_2 extend from 970 (2.1 μm ZnO) to 1700 s^{-1} (1.1 μm ZnO), and no unambiguous trend with the film thickness is observed. The scatter of the mean values is only a factor of 1.7 which is too small to be discussed as a significant change. The apparent differences might result from small deviations in the heating conditions affecting the sheet resistance of the substrate.[20]

These findings serve as a further indication that the decay of the transient photocurrent reflects only the charge transport through the ITO layer. Because the transport through the ZnO layer is much faster than the transport through the substrate, the charge carriers are accumulated at the boundary between the ZnO and the ITO. Because of the porous structure of the ZnO film, the electrolyte solution interpenetrates the particulate ZnO network and forms a double layer with the ITO as well as with the ZnO. Thus, the accumulation of electrons at the outermost part of the substrate might correspond to a charge storage in the double layer of the ITO, and the transport through the substrate might be limited by the discharge of the double layer capacitance. Using a resistance of the ITO of 25 Ω and a capacitance of 10 μF, the rate constant of this process can be estimated to be 4000 s^{-1}. Because the resistance of the whole electrochemical cell and the apparatus contributes also to the net resistance, the actual rate constant for a discharge is most probably smaller than this estimate corresponding well to the value of k_2 obtained from the photocurrent transients.

In the lower part of Figure 7, the corresponding data are depicted for the parameter k_1 which accounts for the transport of the electrons through the ZnO layer. In general, all samples exhibit a similar shape of the data curves. At positive potentials,

the parameter k_1 is constant, whereas it shows a strong increase toward more negative potentials. By comparing the results obtained for different ZnO films, it is found that the rate constants decrease clearly by increasing the film thickness in accordance with the expectation from our model.

Analysis of the Fitting Parameter k_1. To specify the driving force for the charge transport, two processes might be taken into consideration: a diffusion transport or a migration of electrons in the effective electric field applied. Because of the porous nature of the ZnO film and the good shielding of the electrolyte solution interpenetrating the particulate network, an electric field is unlikely to be established. It is more reasonable to assume a charge transport inside the nanoporous film by diffusion. Thus the irregular motion of the electron traversing the ZnO layer can be described by the theory of a random walk. The mean square displacement $\langle x^2 \rangle$ from the starting point denotes the progress of a moving object. In general, this quantity is given at any time t by

$$\langle x^2 \rangle = aDt \tag{5}$$

where D represents the diffusion constant. The parameter a is connected with the directions available for a propagation: For the one-dimensional random walk with an equal probability to propagate in two possible directions, $+x$ and $-x$, a equals 2, and eq 5 is transformed into the Einstein−Smoluchowski equation. To account for other types of propagation, a would have to be changed. Because in a transient photocurrent experiment only the net charge transport through the electrode is detected, no information is given for a lateral component of the electron movement. Thus, it is reasonable to simplify the net transport process as a one-dimensional diffusion (i.e., $a = 2$) yielding an effective diffusion constant D^* for the electrons.

For the ZnO electrode, the root of the mean square distance $\langle x^2 \rangle$ has to be the respective film thickness d which is traversed after the time τ and thus

$$d = \sqrt{\langle x^2 \rangle} = \sqrt{2D^*\tau} \tag{6}$$

The spatial distribution of the moving objects in a random walk follows a Gaussian distribution with the standard deviation $\sigma = (2D^*t)^{1/2} = (\langle x^2 \rangle)^{1/2}$ centered at $x = 0$.[21] Thus, the time τ in a random walk refers to the moment at which 32% of the moving objects have traversed at least the distance $(\langle x^2 \rangle)^{1/2}$, and 68% of the electrons are still inside the ZnO layer. Using eq 4, τ can thus be rewritten as

$$\tau = -\frac{\ln 0.68}{k_1} \tag{7}$$

By combining eqs 6 and 7, one obtains the relationship

$$d = \sqrt{0.77D^*}k_1^{-1/2} \tag{8}$$

According to eq 8, plotting $k_1^{-1/2}$ versus the film thickness should yield a straight line. In Figure 8, such a representation is given for ZnO/ITO electrodes held at different potentials. It can be seen that a linear correlation is obtained justifying the assumption of a diffusion transport process for all potentials applied. At positive potentials, the data curves collapse into a single line indicating an identical transport process. If the potential is shifted in the negative direction, the slopes of these lines decrease.

For all potentials applied, the intersection of these lines with the x axis is virtually the same. The intersection at 260 nm might be interpreted as the minimal thickness for which a finite rise of the photocurrent transient and thus a diffusion process can be observed. This value is about three times the penetration depth of the laser light and corresponds thus to almost complete absorption of the incident light. Therefore, the interpretation of the parameter k_1 describing the charge transport in the nonilluminated part of the ZnO electrode might be confirmed.

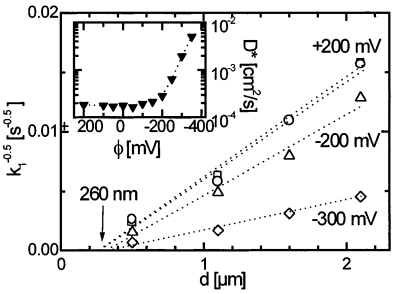

Figure 8. Plot of the reciprocal square root of the fitting parameter k_1 versus the thickness of the ZnO film according to the Einstein−Smoluchowski equation (open symbols). The ZnO electrodes were held at different potentials (square: +200 mV; circle: −100 mV; triangles: −200 mV; diamonds: −300 mV). The broken lines correspond to the respective fits using a linear regression. As denoted by the arrow, all lines intersect with the x axis at the same thickness. The inset depicts the effective diffusion constant D^* for the electron transport through the particulate ZnO films as calculated from the slopes of the lines.

From the slopes of these straight lines as determined by a linear regression, the effective diffusion constant D^* was calculated with respect to eq 8 for each potential applied. The thus obtained D^* is shown in the inset of Figure 8 on a logarithmic scale. At positive potentials, the diffusion constant is independent of the actual potential having an average value of 1.7×10^{-4} cm^2/s. For a comparison with the diffusion constant in macroscopic ZnO single crystals, this quantity can be calculated from an electron mobility of 200 cm^2/sV (300 K)[22] using the Einstein relationship for nondegenerate semiconductors[22] to be about 5.2 cm^2/s. The value obtained for the nanoparticulate system is thus smaller by more than 4 orders of magnitude indicating a charge transport process which is completely different in both systems. For ZnO electrodes consisting of particles 5 nm in size, Meulenkamp reports diffusion constants between 2.5×10^{-3} and 2.5×10^{-5} cm^2/s.[23] The effective diffusion constants obtained from our experiments correspond very well with these values. Because similar results were extracted from transient photocurrents of particulate TiO_2 electrodes, Meulenkamp proposes that the actual value of the diffusion coefficient might rather reflect the particulate structure of the films than the material itself.

As the potential is shifted in a negative direction, D^* becomes considerably larger until it is increased by a factor of 30 at −350 mV. At potentials even more negative, no information could be extracted from the rise of the photocurrent transients due to the limitations of the measurement apparatus. Because the diffusion coefficient describes the proportionality between the driving force of a transport and the resulting flux, D^* should be independent of the electrode potential for porous systems. However, as it might be seen from the linear relationship between the d and $k_1^{-1/2}$ even at negative potentials applied, the transport process itself is still a diffusion. The increase of D^* might reflect the increase of the number of electronic states which are occupied in the charge transport as the potential approaches the potential of the conduction band. Because the electron transport through the ZnO layer takes place via the empty states with the lowest energy, the rate of an electron transport through the porous film is expected to increase at more

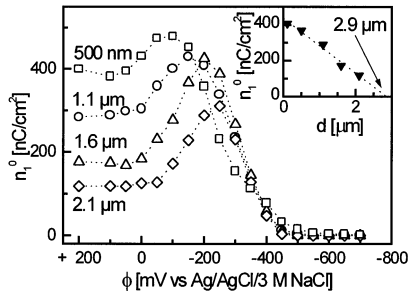

Figure 9. Fitting parameter n_1^0 for ZnO electrodes having different film thicknesses (500 nm, 1.1 μm, 1.6 μm, and 2.1 μm). This parameter corresponds to the amount of charge whose transport is accounted for by the simple model. The inset shows the relationship between the mean value of n_1^0 obtained for positive potentials and the thickness of the ZnO layer.

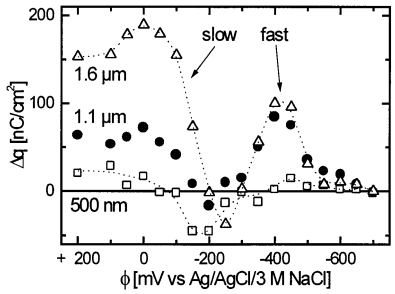

Figure 10. Difference between the total charge flown (integral of the photocurrent transient) and the amount of charge which is described by the phenomenological model for three ZnO electrodes having different thicknesses (500 nm, 1.1 μm, and 1.6 μm).

negative potentials.[24] Within a mechanistic picture, this increase of D^* might be explained in several ways: Because the transport is affected even at potentials being more positive than the potential of the conduction band, empty electronic states which are located below the conduction band might be involved in the charge transport between adjacent particles. These transitions might occur directly via these trap states or via the conduction band after a detrapping has taken place. Because in both cases the traps become more shallow as the potential is shifted in negative direction, the rate constant of the net transport increases. Furthermore, the existence of potential barriers between the particles could be taken into account which determine the rate of the electron transport through the ZnO film. By applying negative potentials, the height of these barriers decreases facilitating a charge transport. However, the present experimental data are not sufficient for a more detailed analysis of the underlying mechanism.

Analysis of the Fitting Parameter n_1^0. In Figure 9, the fitting parameter n_1^0 is shown for ZnO samples having film thicknesses of 500 nm, 1.1 μm, 1.6 μm, and 2.1 μm, respectively. All data curves have basically similar shapes differing only at potentials positive from the peak. Because the only parameter varied was the thickness of the nonilluminated part of the ZnO layer, two conclusions can be drawn from the similar shape of these curves at potentials negative of −200 mV. First, it can be deduced that no significant recombination inside the nonilluminated volume of the ZnO has to be considered during the charge transport, because such a recombination should affect strongly the amount of charge carriers collected at the back contact for potentials between −200 and −600 mV. This finding is supported by transient photopotential experiments performed under open-circuit conditions (not shown here). These measurements show that the decay of the photopotential is very slow (with a time constant of 15 s) thus indicating only a discharge through the external circuit of the oscilloscope. A decay due to a reaction of the electrons with the electrolyte solution was not observed.

Second, the initial charge separation after the laser pulse shows no influence of the ZnO film thickness at negative potentials applied. Hence, it is unlikely to assume a potential drop across the thickness of the ZnO layer as it was observed by Zaban and co-workers for particulate TiO_2 electrodes.[25]

By shifting the potential from that at the apparent peak in the positive direction, the parameter n_1^0 decreases until it reaches a constant value at positive potentials. This decrease is bigger the thicker the ZnO was. The inset in Figure 9 shows a linear relationship between the mean value of n_1^0 obtained for positive potentials and the thickness of the ZnO film. Thus, the competing processes which account for the drop of n_1^0 at positive potentials has to scale linearly as well. The intersection of the line in the inset with the x axis is found to be 2.9 μm. For films thicker than 2.9 μm, no electron diffusion might be observed in the transient photocurrents at positive potentials applied, because all charge carriers are transported in a slower transport process.

To achieve a better understanding of the underlying effects for the drop of the n_1^0, the difference Δq between the charge n_1^0 (according to the transport described by eq 4) and the total charge flown (as obtained by integration of the photocurrent) was calculated. The resulting differences are given in Figure 10 (in order to obtain a better presentation of Δq for the thinner electrodes, the corresponding data for the 2.1 μm electrode is omitted). At positive potentials, all samples show a positive Δq indicating that additional charge carriers reach the back contact which are not accounted for by the phenomenological model. The amount of this charge increases by increasing the film thickness. As stated above, this contribution corresponds to a slow transport process (in the millisecond time domain). This additional current scales linearly with the thickness of the ZnO layer and might thus reflect a transport process through the ZnO layer which proceeds via deep trap states. Once an electron has been trapped in such states, it can no longer contribute to a transport via conduction band states as described by eq 4. As the potential is shifted in the negative direction, these trap states are filled with electrons via the back contact and the charge transport occurs only using unoccupied states at higher energies. Hence, no contribution of this slow transport to the photocurrent is observed at negative potentials. According to Figure 10, the potential corresponding to these deep traps is found to be about −100 mV. Thus, these trap states are located about 400 meV below the conduction band states.

For TiO_2 films, a comparable slow transport via deep traps has been proposed by various authors: By analyzing the photocurrent transients of polycrystalline TiO_2 electrodes, a transport mechanism requiring at least two different kinds of traps was proposed by Schwarzburg and Willig.[26] Additionally, studies reported by Solbrand and co-workers gave further indication for the existence of this kind of transport occurring in thick TiO_2 films.[5] Similar conclusions were drawn from the results of intensity-modulated photocurrent measurements by de Jongh and Vanmaekelbergh.[27]

TiO_2 particles are known to contain a large quantity of trap states.[11,28] Thus, it is most likely that an electron diffusion through such electrodes is dominated by the trapping/detrapping kinetics of the propagating electrons. For the ZnO/ITO electrodes employed in our study, only a part of the charge carriers are transported via deep traps whose magnitude has shown to be dependent on the thickness of the films and on the potential

applied. On the other hand, the electrodes examined in most studies on TiO_2 were significantly thicker than our samples. It might be expected even for ZnO electrodes having a thickness of more than 2.9 μm that mainly a slow electron transport takes place. Thus, it is not clear whether the differences between the findings in particulate TiO_2 electrodes and our results in ZnO reflect an effect of the material or simply of the film thickness.

For the ZnO samples examined in our study, the fraction of charge carriers which undergoes such a slow transport is for the thickest sample (2.1 μm) as high as 50% of the total charge flown. To account for this additional pathway of a charge transport, a mathematically more extensive model might be suitable, as it was shown for particulate TiO_2 by performing numerical Monte Carlo simulations[10,11] or by solving the diffusion equation for the respective boundary conditions.[4,5] However, the latter approach is much simpler for particulate TiO_2 electrodes because in these systems no contribution of the substrate to the temporal evolution of the photocurrents was found. On the other hand, for the ZnO/ITO electrodes, the transport through the ITO has to be considered. Therefore, two coupled differential equations are required in order to describe the charge transport. and it is questionable whether analytical solutions can be obtained.

The difference Δq observed at potentials negative of -300 mV is positive. This charge is ascribed to a fast contribution of the initial photocurrent. For the thinnest ZnO film, the difference is very small, whereas the thicker samples show larger and similar deviations. Thus, the question arises whether this component is simply not present in the thinner ZnO films or whether it is already taken into account by the fitting procedure. It is seen in Figure 9 that the n_1^0 of the 500 nm ZnO film exhibits a slight shoulder at potentials between -250 and -550 mV. Thus, it is most likely that the additional current is already accounted for by the fitting procedure. Because a data fit is only affected by data which are of the same order of magnitude as the main component of the data, the rate constant corresponding to the additional current must be of the same order of magnitude as k_1 for the 500 nm ZnO electrode. For the thicker samples, such a shoulder is not observed. Thus, the rate of a transport via the additional channel must be different from the respective k_1. Consequently, the additional contribution is most likely to be independent of the thickness of the ZnO layer and might reflect a process only occurring in the illuminated part of the ZnO, e.g., a reorganization of the electrolyte double layer in the illuminated volume as it was proposed to apply for TiO_2 by Solbrand and co-workers.[4] However, for a more detailed analysis of this component, the available information is not sufficient.

Conclusion

For ZnO/ITO electrodes, the transient photocurrent $i(t)$ consists of three different components corresponding to $i(t) = i_I(t) + i_D(t) + i_T(t)$. The fast initial component $i_I(t)$ is observed immediately after the laser pulse and exhibits no effect of the film thickness. This component arises probably from a reorganization of the double layer after a fast initial electron transport. The slow charge transport $i_T(t)$ is observed at long times after the laser pulse only for positive potentials applied. It is explained as a slow transport channel for the photoexcited electrons via deep trap states 400 meV below the conduction band edge. The simple model presented in this study does not account for both of these processes explicitly. The current component $i_D(t)$ describes the main part of the shape of the photocurrent transient. The model presented offers a simple way for the interpretation of this current component by distinguishing the subsequent transport processes in the ITO and in the ZnO layer. The only assumptions made are the restriction to a one-dimensional transport pathway and a good ohmic contact between the two points in which $\tilde{N}_1$ and N_2 are balanced. Though other evaluation techniques require additional assumptions or boundary conditions, this information is included implicitly in the fitting parameter n_1^0. In detail, these processes are the geminate recombination (radiative as well as nonradiative) and the initial charge separation which takes place on a much faster time scale and thus virtually before a net charge transport is monitored.

The transport through the substrate might be described as a discharge of the charge accumulated at the boundary between the ITO and the ZnO through the net resistance of the cell. The contribution of the ZnO was interpreted in terms of an electron diffusion through the electrode via conduction band or shallow trap states. By applying the theory of a random walk, an effective diffusion constant for the electrons is obtained.

The simple approach lacks detailed information about the temporal evolution of the spatial charge carrier distribution, as it might be gained from other approaches by solving the diffusion equation. The simplicity of the model presented in this study counteracts this deficiency encouraging its application in the analysis of transient photocurrents.

Furthermore, by identifying the driving force of the transport process, the actual mechanism is still unknown, by which the electrons are transferred to adjacent particles. To specify the underlying process, temperature dependent measurements of the photocurrent transients have to be performed. The successful analysis of the current transients in nanoporous ZnO electrodes motivates strongly further steps into this direction.

References and Notes

(1) Hagfeldt, A.; Grätzel, M. *Chem. Rev.* **1995**, *95*, 49.
(2) Hoffmann, M. R.; Martin, S. T.; Choi, W.; Bahnemann, D. W. *Chem. Rev.* **1995**, *95*, 69.
(3) Hoyer, P.; Weller, H. *J. Phys. Chem.* **1995**, *99*, 14096.
(4) Solbrand, A.; Lindström, H.; Rensmo, H.; Hagfeldt, A.; Lindquist, S.-E.; Södergren, S. *J. Phys. Chem. B* **1997**, *101*, 2514.
(5) Solbrand, A.; Henningsson, A.; Södergren, S.; Lindström, H.; Hagfeldt, A.; Lindquist, S.-E. *J. Phys. Chem. B* **1999**, *103*, 1078.
(6) Bisquert, J.; Garcia-Belmonte, G.; Fabregat-Santiago, F.; Ferriols, N. S.; Bogdanoff, P.; Pereira, E. C. *J. Phys. Chem. B* **2000**, *104*, 2287.
(7) Dloczik, L.; Ileperuma, O.; Lauermann, I.; Peter, L. M.; Ponomarev, E. A.; Redmond, G.; Shaw, N. J.; Uhlendorf, I. *J. Phys. Chem. B* **1997**, *101*, 10281.
(8) Peter, L. M.; Ponomarev, E. A.; Franco, G.; Shaw, N. J. *Electrochim. Acta* **1999**, *45*, 549.
(9) de Jongh, P. E.; Meulenkamp, E. A.; Vanmaekelbergh, D.; Kelly, J. J. *J. Phys. Chem. B* **2000**, *104*, 7686.
(10) Nelson, J. *Phys. Rev. B* **1999**, *59*, 15374.
(11) van de Lagemaat, J.; Frank, A. J. *J. Phys. Chem. B* **2001**, *105*, 11194.
(12) Bahnemann, D. W.; Kormann, C.; Hoffmann, M. R. *J. Phys. Chem.* **1987**, *91*, 3789.
(13) Spanhel, L.; Anderson, M. A. *J. Am. Chem. Soc.* **1991**, *113*, 2826.
(14) Hoyer, P.; Eichberger, R.; Weller, H. *Ber. Bunsen-Ges. Phys. Chem.* **1993**, *97*, 630.
(15) Noack, V.; Eychmüller, A. *Chem. Mater.* **2002**, *14*, 1411.
(16) Hotchandani, S.; Kamat, P. V. *J. Electrochem. Soc.* **1992**, *139*, 1630.
(17) Scher, H.; Montroll, E. W. *Phys. Rev. B* **1975**, *12*, 2455.
(18) Noack, V.; Weller, H.; Eychmüller, A., submitted.
(19) Mauser, H. *Formale Kinetik*; Bertelsmann Universitätsverlag: Düsseldorf, Germany, 1974; p 78.
(20) Jarzcebski, Z. M. *Phys. Stat. Sol. (A)* **1982**, *71*, 13.
(21) Bockris, J. O. M.; Reddy, A. K. N. *Modern Electrochemistry*; Plenum Press: New York, 1970; Vol. 1, p 332.
(22) Sze, S. M. *Physics of Semiconductor Devices*, 2nd ed.; John Wiley & Sons: New York, 1981.
(23) Meulenkamp, E. A. *J. Phys. Chem. B* **1999**, *103*, 7831.

(24) From a kinetic point of view, the transport might be interpreted as a bimolecular reaction between an electron inside particle 1 and an empty state (#) inside the adjacent particle 2 ($e^-_1 + \#_2 \rightarrow \#_1 + e^-_2$), which might be rewritten as a pseudo-first-order process by including the number of the empty states in the net rate constant. Consequently, the net rate constant is altered when the potential is shifted in the negative direction.

(25) Zaban, A.; Meier, A.; Gregg, B. A. *J. Phys. Chem. B* **1997**, *101*, 7985.
(26) Schwarzburg, K.; Willig, F. *Appl. Phys. Lett.* **1991**, *58*, 2520.
(27) de Jongh, P. E.; Vanmaekelbergh, D. *J. Phys. Chem. B* **1997**, *101*, 2716.
(28) Könenkamp, R. *Phys. Rev. B* **2000**, *61*, 11057.